0026-895X/01/6004-790–796$3.00
MOLECULAR PHARMACOLOGY
Copyright © 2001 The American Society for Pharmacology and Experimental Therapeutics
Mol Pharmacol 60:790–796, 2001

Vol. 60, No. 4
964/931954
Printed in U.S.A.

The Kinetics of Inhibition of Nicotinic Acetylcholine Receptors by (+)-Tubocurarine and Pancuronium

INGOBERT WENNINGMANN and JAMES P. DILGER

Klinik für Anästhesiologie, Universität Bonn, Bonn, Germany (I.W.); and Departments of Anesthesiology and Physiology & Biophysics, State University of New York at Stony Brook, Stony Brook, New York

Received March 19, 2001; accepted July 3, 2001

This paper is available online at http://molpharm.aspetjournals.org

ABSTRACT

Equilibrium conditions of neurotransmitter concentration and receptor binding are never achieved during synaptic transmission at the neuromuscular junction. Thus, it is important to determine the binding kinetics of drugs that act this synapse. Previous determinations of the dissociation rate of (+)-tubocurarine have produced inconsistent results ranging from 0.1 to 4000/s. Here, we used a direct approach to measure association (ℓ_{on}) and dissociation (ℓ_{on}) rates for two competitive antagonists (clinically used as nondepolarizing muscle relaxants), pancuronium and (+)-tubocurarine, at nicotinic acetylcholine receptors (nAChR). We made macroscopic current recordings from outside-out patches of BC3H-1 cells expressing embryonic mouse muscle nAChR. We used a three-tube rapid perfusion system to make timed applications of antagonists and acetylcholine to the patch. We made independent measurements of the equilibrium inhibition (IC_{50}) and the kinetics of onset and recovery of antagonist inhibition at 20 to 23°C. Rate constants were calculated from the predictions of a single (high-affinity) site model of competitive inhibition. For pancuronium: $IC_{50} = 5.5 \pm 0.5$ nM (mean ± S.D.), $\ell_{on} = 2.7 \pm 0.9 \times 10^8$ M^{-1} s^{-1}, $\ell_{off} = 2.1 \pm 0.7 \times 10^8$/s. For (+)-tubocurarine: $IC_{50} = 41 \pm 2$ nM, $\ell_{on} = 1.2 \pm 0.2 \times 10^8$ M^{-1} s^{-1}, $\ell_{off} = 5.9 \pm 1.3$/s. The kinetic results are consistent with the equilibrium results in that ℓ_{off}/ℓ_{on} is in good agreement with the IC_{50} values. All differences between the antagonists are significant at the $p < 0.001$ level. The higher affinity of pancuronium is caused by a faster association rate (2.2-fold) coupled with a slower dissociation rate (2.8-fold). The association rates of both antagonists are comparable with or greater than the association rate for acetylcholine binding to nAChR.

Transmission at fast chemical synapses is a fundamental process in the central and peripheral nervous systems. The best-studied example is the neuromuscular junction. The nicotinic acetylcholine receptor (nAChR) mediates rapid synaptic transmission by increasing the conductance of the postsynaptic cell membrane in response to nerve-released ACh. High speed is achieved because both the receptor and the ion channel are parts of a single protein molecule.

One complicating feature of neuromuscular transmission is the presence of multiple binding sites for ACh. There are two nonidentical ACh binding sites on the receptor itself. The low affinity agonist blocking site within the pore of the channel is a third site. Acetylcholinesterase also recognizes ACh. Extrasynaptic muscle ACh receptors and presynaptic neuronal ACh receptors provide additional ACh binding sites. A neuronal subtype ACh receptor has been found on the postsynaptic membrane as well (Tsuneki et al., 1995). The presence of competitive inhibitors (muscle relaxants) to block movement during surgery introduces yet another molecule that can bind to the ACh receptors. Finally, because ACh is rapidly released and hydrolyzed, equilibrium conditions are never reached within the synapse.

A detailed description of the structure and function of the ACh receptor is emerging from several areas of investigation. Electron microscopy of receptors from *Torpedo californica* electroplax membranes has provided structural images at 4.6-Å resolution (Miyazawa et al., 1999) and has revealed structural differences between the open and closed states (Unwin, 1995). Site-directed mutagenesis studies have identified particular amino acids involved in agonist and antagonist binding (Arias, 2000) and ion selectivity and permeation (Corringer et al., 2000). High-resolution, single-channel measurements have determined the rate constants for transitions between states of the receptor (Colquhoun and Sakmann, 1981; Zhang et al., 1995; Maconochie and Steinbach, 1998) and lower limits on the speed of channel opening (Maconochie et al., 1995; Parzefall et al., 1998). Patch-clamp recording during rapid application of agonist has provided a controlled way of mimicking the physiological exposure of

This research was supported in part by National Institute of General Medical Sciences Grant GM42095, the Department of Anesthesiology, State University of New York at Stony Brook, and the Klinik für Anästhesiologie, Universität Bonn, Germany. Parts of this work were presented in abstract form: *Anesthesiology* **91:**A1046, 1999 and *Anasthesiol Intensivmed Notfallmed Schmerzther* **35:**607–608, 2000.

ABBREVIATIONS: nAChR, acetylcholine receptor; ACh, acetylcholine; ECS, extracellular solution.

ACh receptors to ACh (Brett et al., 1986; Franke et al., 1987; Maconochie and Knight, 1989).

Measurements of the kinetics of agonist association suggest that they bind more slowly than predicted from simple diffusion (Gutfreund, 1972; Zhang et al., 1995). Structural studies of *T. californica* nAChR suggest the existence of ACh binding pockets accessible through narrow tunnels in the channel wall (Miyazawa et al., 1999). Diffusion through these tunnels may be the limiting factor for ACh association. It would be interesting to see if this is also true for antagonists. The binding affinity of the prototypical antagonist, (+)-tubocurarine, has been determined as 400 nM in frog muscle (Jenkinson, 1960) and 250 nM in rat muscle (Colquhoun and Rang, 1976). However, measurements of the kinetics of antagonist binding have produced inconsistent results. Estimates of the association rate of the prototypical antagonist, (+)-tubocurarine range from 10^9 M^{-1} s^{-1} (Colquhoun and Sheridan, 1982; Le Dain et al., 1991) to 5×10^5 M^{-1} s^{-1} (Bufler et al., 1996). Similarly, estimates of the dissociation rate range from 1000 to 4000/s (Colquhoun and Sheridan, 1982; Le Dain et al., 1991) to 0.1/s (Bufler et al., 1996). We undertook this study to try to resolve these discrepancies. Pancuronium was also studied as an example of a higher affinity competitive antagonist in current use as a neuromuscular blocking agent.

Materials and Methods

We studied the embryonic mouse muscle nicotinic ACh receptors expressed in clonal BC3H-1 cells. The cells were cultured as described previously (Sine and Steinbach, 1984). To prepare cells for patch-clamp recording, the culture medium was replaced with an "extracellular" solution (ECS) containing 150 mM NaCl, 5.6 mM KCl, 1.8 mM $CaCl_2$, 1.0 mM $MgCl_2$, and 10 mM HEPES, pH 7.3. Patch pipettes were fabricated from borosilicate glass and firepolished. They were filled with a solution consisting of 140 mM KCl, 5 mM EGTA, 5 $MgCl_2$, 10 (+)-glucose, and 10 mM HEPES, pH 7.3, and had resistances of 3 to 5 MΩ. An outside-out patch (Hamill et al., 1981) with a seal resistance of 5 GΩ or greater was obtained from a cell and moved into position at the outflow of a perfusion system. The perfusion system [modified from Liu and Dilger (1991)] consisted of solution reservoirs; computer-controlled, solenoid-driven pinch valves; and a three-tube device immersed in the culture dish. The three tubes were made of glass and were attached with epoxy so that they were coplanar and at 45° angles from each other. One tube was connected to a reservoir containing ECS without agonist (control), the second arm was connected to a reservoir containing ECS with 100 μM ACh (agonist solution), and the third arm was connected to a reservoir containing ECS with either (+)-tubocurarine or pancuronium (test solution) [(+)-tubocurarine chloride and pancuronium bromide; Sigma Chemical Co., St. Louis, MO]. In the resting position, control solution perfused the patch. The perfusion system allowed for a rapid solution exchange within 100 to 200 μs between each tube. When making onset- or recovery experiments (see below), we could reliably achieve a minimum duration of 10 ms for the second solution. We tested the timing systematically using an open electrode perfused with solutions of different ionic strength and confirmed the optimal position of the electrode frequently using open electrode tests.

The currents flowing during exposure of the patch to ACh were measured with a patch clamp amplifier (EPC-9; List Medical, Darmstadt, Germany), filtered at 3 kHz (3 db frequency, eight-pole Bessel filter), digitized and stored on the hard disk of a laboratory computer. Data analysis was performed off-line as described previously (Dilger et al., 1997). Experiments were performed at room temperature (20–23°C.). We recorded current responses (at −50 mV) during 100- to 200-ms applications (at 5-s intervals and sampled at 100–200 μs per point) of ECS containing 100 μM ACh, a concentration that opens about 93% of the nAChR channels from BC3H-1 cells (Dilger and Brett, 1990). We subsequently used this test solution to quantify loss of channel activity.

To determine antagonist onset kinetics, we equilibrated the patch with ECS, perfused with antagonist for a variable time interval (10–1500 ms) and then measured the current response to 100- to 200-ms applications of 100 μM ACh to assess the fraction of antagonist-free channels. To determine recovery kinetics, we equilibrated the patch with antagonist, removed antagonist for variable time intervals (10–1500 ms), and then applied ACh. We repeated this with various concentrations of antagonist. The association and dissociation rate constants were calculated from the assumption of a single-site binding model; this corresponds to the higher affinity antagonist binding site (Fletcher and Steinbach, 1996). Responses of the patch to 100 μM ACh applications were measured before and after each onset/recovery protocol to test for loss of channel activity. Data were accepted when these two differed by less than 10%. The ensemble mean current was calculated from 10 to 20 individual current traces. Under most circumstances, mean currents were fit to single exponential functions to obtain peak and steady-state current values and a time constant of the decay caused by desensitization. At high concentrations of (+)-tubocurarine, the currents had a biphasic time course (see Fig. 2). In these cases, the currents were fit to a biexponential function to determine the current at the end of the initial activation phase. The initial mean current was defined as the current after the initial activation phase. We calculated the ratio of this current in the presence and absence of the antagonists.

Data are expressed and graphed as mean ± S.D. To facilitate statistical comparison, we performed curve fits using all data points rather than the mean values. Parameters derived from curve fitting are expressed as best-fit values ± S.D. Statistical comparisons are made using an unpaired two-tailed t test. To compare association rates, we performed the t test based on the linear regression analysis (Igor Pro software; Wavemetrics, Lake Oswego, OR) of the reciprocal of the onset time constant versus antagonist concentration (see eq. 3). This results in a mean value and S.D. of the slope.

Results

Competitive Antagonism under Equilibrium Conditions. In these experiments, we equilibrated the patch with various concentrations of the antagonist for >1 min before applying a mixture of 100 μM ACh and the antagonist. Figure 1a shows examples of currents seen in a single patch with 0, 3, and 30 nM pancuronium. The control trace exhibits a rapid activation phase whereas 100 μM ACh activates about 93% of the receptors and a desensitization phase with a time constant of 53 ms. The main effect of pancuronium is to reduce the peak current. The decay phase is still described by a single exponential function, but the decay rate is slowed at high concentrations of pancuronium (the decay time constant was 200 ms at 30 nM.). Similar effects are seen with low concentrations of (+)-tubocurarine (Fig. 1b). However, at high concentrations of (+)-tubocurarine, the current exhibits a biphasic time course after the initial activation phase. Figure 2 shows an example of a current in the presence of 200 nM (+)-tubocurarine along with a 2-exponential fitting function that describes the biphasic time course.

We used the current value after the initial activation phase in the presence of antagonist, I_{Drug}, to represent the equilibrium inhibition. The ratio of these currents to the control peak currents, I_0, is plotted as a function of antagonist con-

centration in Fig. 3. These concentration-response curves were fit to a Hill equation

$$\frac{I_{Drug}}{I_0} = \frac{IC_{50}{}^{n_H}}{IC_{50}{}^{n_H} + [Drug]^{n_H}} \quad (1)$$

where [Drug] is the antagonist concentration, IC_{50} is the concentration for 50% inhibition, and n_H is the Hill coefficient. The results are shown in Table 1. Pancuronium is about eight times more potent at inhibiting the nAChR than is (+)-tubocurarine (IC_{50} = 5.5 nM and 42 nM, respectively). The Hill slopes are close to 1.0, which suggests that the inhibition is dominated by the high affinity binding site. To determine whether the difference in Hill slope was significant, we reanalyzed the data by calculating the IC_{50} and n values for each patch (those for which at least two concentrations of antagonist were studied). The results [n = 1.13 ± 0.24 (10 patches using (+)-tubocurarine) and n = 1.17 ± 0.17 (6 patches using pancuronium)] are not statistically different. In an attempt to extract some information about the low-affinity binding sites, we also fit the data to a two-site model:

$$\frac{I_{Drug}}{I_0} = \frac{L_1L_2}{L_1L_2 + L_1[Drug] + L_2[Drug] + [Drug]^2} \quad (2)$$

where L_1 and L_2 are the affinities of the two binding sites. For pancuronium, the low-affinity site was not well determined by the data (Table 1). The eq. 2 fitting routine did not converge for (+)-tubocurarine; this is not surprising because this equation cannot describe data that is characterized by a Hill coefficient <1.0.

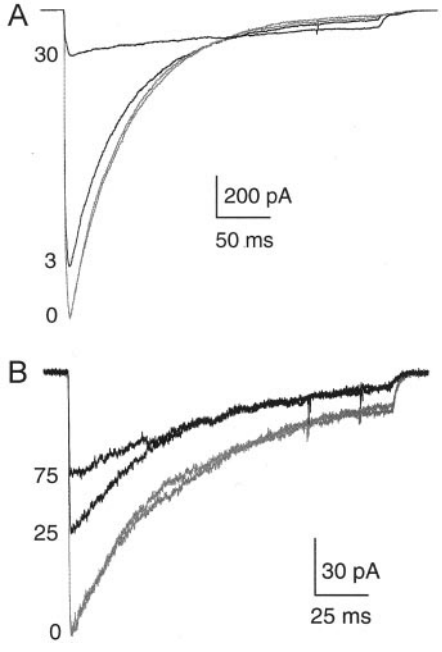

Fig. 1. A, the effects of 3 and 30 nM pancuronium on currents evoked by rapid perfusion of 100 μM ACh to an outside out patch. V = −50 mV. Two control curves are shown. The traces for 30 nM and the corresponding control were scaled by a factor of 1.072 to compensate for loss of channel activity during this experiment. B, the effects of 25 and 75 nM (+)-tubocurarine on currents evoked by rapid perfusion of 100 μM ACh to an outside out patch. V = −50 mV. Two control curves are shown. The traces for 25 nM and the corresponding control were scaled by a factor of 1.094 to compensate for loss of channel activity during this experiment (there were 55 min between the two determinations).

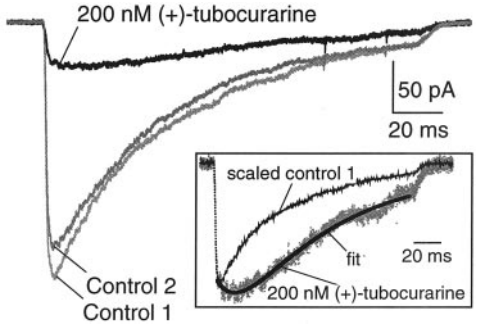

Fig. 2. An example of the biphasic current response to 100 μM ACh in the presence of 200 nM (+)-tubocurarine. The inset shows the two exponential fit used to characterize such responses. The fit functions were (currents in pA, time in ms; control fits not shown): control 1, I(t) = −16 −245*exp(−t/47.1); 200 nM (+)-tubocurarine, I(t) = −2.61 −65.1*exp(−t/71.3) + 28.8*exp(−t/17.8); control 2, I(t) = −13.6 −227*exp(−t/45.8)

The Kinetics of Competitive Antagonism. We speculated that the biphasic current response seen with (+)-tubocurarine but not with pancuronium might be related to the rate at which the drug dissociates from the receptor. If (+)-tubocurarine were to dissociate on the 100-ms time scale and pancuronium were to dissociate more slowly, the slow rise in current might be caused by ACh binding to receptors previously bound by (+)-tubocurarine. Such behavior has been predicted (Rang, 1966; Aoshima et al., 1992). Our first experimental approach to determining the kinetics of (+)-tubocurarine is illustrated in Fig. 4. Channels were activated by 3 μM ACh, a concentration that induces only a small amount of desensitization within 200 ms. Equilibrium application of 500 nM (+)-tubocurarine inhibited the current to 15% of control. Simultaneous application of ACh and (+)-tubocurarine produced a time-dependent current that decayed from the control level to the equilibrium level with a time constant of 16 ms (Fig. 4A.). Equilibration with (+)-tubocurarine followed by perfusion of ACh without (+)-tubocurarine produced a relaxation from the equilibrium to the control level with a time constant of 75 ms (Fig. 4B.). These two numbers provided a first estimate of the kinetics of (+)-tubocurarine association and dissociation. This experimental approach is

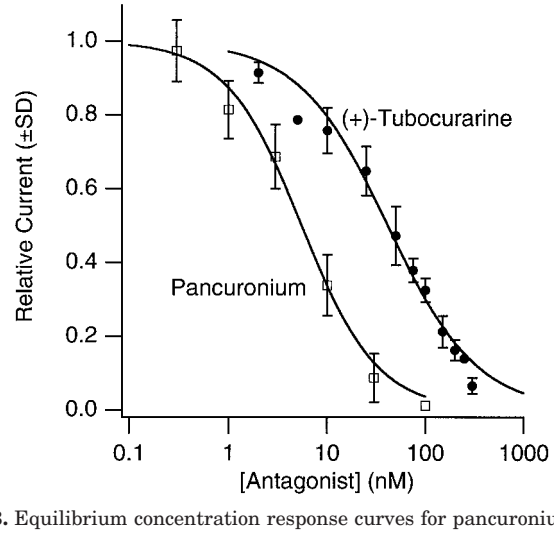

Fig. 3. Equilibrium concentration response curves for pancuronium and (+)-tubocurarine on nAChR from BC3H-1 cells. The solid lines are fits of eq. 1 to the data. The fitting parameters are given in Table 1.

limited in that fast relaxation times are distorted by the onset of the ACh-activated currents and slow relaxation times are distorted by desensitization.

We then used all three tubes of the perfusion apparatus to measure the kinetics of antagonist association and dissociation directly. Figure 5A shows examples from an onset experiment in which receptors are equilibrated with 20 nM pancuronium for various time intervals and then perfused with 100 μM ACh and 20 nM pancuronium to assess the fraction of antagonist-free receptors. Half of the total inhibition at this concentration is achieved with a ~150-ms exposure to pancuronium. Figure 5b shows the data using the onset protocol with 150 nM (+)-tubocurarine. Here 50% of the total inhibition at this concentration is achieved already after 43 to 60 ms of exposure to (+)-tubocurarine. Figure 6 shows the results of recovery experiments with 20 nM pancuronium (Fig. 6a) and 150 nM (+)-tubocurarine (Fig. 6b). For both antagonists, the time course of recovery is slower than that of onset. Recovery is slower with pancuronium than with (+)-tubocurarine. The data from Figs. 5 and 6 were analyzed in terms of the fractional current after the initial activation phase and plotted as a function of the exposure or removal time interval (Fig. 7). The data were fit to a single exponential function; the time constants are indicated on the graphs. The kinetics of (+)-tubocurarine is considerably faster than the kinetics of pancuronium.

We used a two-state model to describe the binding of antagonist with the receptor in the absence of ACh (agonist is not present when the antagonist is being exposed or removed from the patch).

$$C + R \underset{\ell_{off}}{\overset{[Drug]\,\ell_{on}}{\rightleftharpoons}} CR \qquad (3)$$

R represents the receptor and C represents the competitive antagonist. The association (ℓ_{on}) and dissociation (ℓ_{off}) rate constants are related to the time constants for onset (τ_{on}) and recovery (τ_{off}) kinetics by (Hill, 1909)

$$\tau_{on} = \frac{1}{\ell_{on}[\text{Drug}] + \ell_{off}} \qquad (4)$$

$$\tau_{off} = \frac{1}{\ell_{off}} \qquad (5)$$

The equilibrium binding constant can be calculated as $L_{eq} = \ell_{off}/\ell_{on}$.

Figure 8 shows the dependence of onset- and recovery rates on antagonist concentrations and fits to eqs. 4 and 5. The results are summarized in Table 1. The association rates for (+)-tubocurarine and pancuronium differ by a factor of 2.2 (2.7 and 1.2 $\times$ 10^8 M^{-1} s^{-1} for pancuronium and (+)-tubocurarine, respectively). These are significantly different with $p < 0.001$ (t test; see *Materials and Methods*). There is good agreement between the dissociation rates determined from onset experiments with those from recovery experiments, but the values from the recovery experiments are less variable. There is an even greater difference in the dissociation rates of the two antagonists; (+)-tubocurarine dissociates 2.8 times faster than pancuronium ($p < 0.001$). The average dwell time for (+)-tubocurarine binding is 170 ms; the dwell time is 480 ms for pancuronium. The ratio of the dissociation to association rate constants is in good agreement with the IC_{50} values determined from equilibrium experiments (Table 1). Both dissociation and association rates contribute to the difference in affinity between the two antagonists.

Discussion

(+)-Tubocurarine and pancuronium are potent neuromuscular blockers used during general anesthesia to provide muscle relaxation. Both drugs have a long history of in vitro and in vivo investigations.

We examined the effects of these antagonists on outside-out patches containing embryonic mouse nAChRs using a two-tube protocol to measure equilibrium inhibition by antagonists. We found IC_{50} values of 5.5 and 41 nM for pancuronium and (+)-tubocurarine, respectively. Our data did not allow us to determine the low affinity constants with any precision. These results are in good agreement with published data on BC_3H1 cells and the QF18 cell line expressing embryonic mouse nAChRs. Bungarotoxin displacement experiments on BC_3H1 cells reveal pancuronium affinities of 9.1 and 69 nM (Sine and Taylor, 1981). Similar experiments on QF18 cells reveal pancuronium affinities of 8 and 95 nM and (+)-tubocurarine affinities of 71 and 1100 nM (Steinbach and Chen, 1995; Fletcher and Steinbach, 1996). Functional measurements reveal similar affinities. In BC_3H1 cells, Na^+ permeability was inhibited by 7.4 nM pancuronium with a Hill coefficient of 1.16 (Sine and Taylor, 1981). In QF18 cells, ion currents were inhibited by 5 nM pancuronium with a Hill coefficient of 1.23 (Fletcher and Steinbach, 1996) and 56 nM (+)-tubocurarine with a Hill coefficient of 1.06 (Steinbach and Chen, 1995).

TABLE 1

Equilibrium and kinetic parameters for pancuronium and (+)-tubocurarine obtained from fitting the data in Figs. 3 and 8

The two binding site model (eq. 2) did not converge for the (+)-tubocurarine data. Residency time and ℓ_{off}/ℓ_{on} are calculated using the value of ℓ_{off} determined from recovery experiments. The number of original data points (before averaging by concentration) is given in parentheses.

	Pancuronium	(+)-Tubocurarine
IC_{50} (nM) (equilibrium)	5.5 ± 0.5 (24)	41 ± 2 (41)*
Hill coefficient (equilibrium)	1.13 ± 0.10	0.95 ± 0.05
L_1,L_2 (nM) (two-site model equilibrium)	6.7 ± 1.2	N.A.
	36 ± 32	N.A.
ℓ_{on} (s^{-1} M^{-1}) (onset)	(2.7 ± 0.9) × 10^8 (14)	(1.2 ± 0.2) × 10^8 (11)*
ℓ_{off} (s^{-1}) (onset)	1.9 ± 1.2 (14)	6.8 ± 2.2 (11)*
ℓ_{off} (s^{-1}) (recovery)	2.1 ± 0.7 (12)	5.9 ± 1.3 (8)*
Residency time (ms) $1/\ell_{off}$	480	170
ℓ_{off}/ℓ_{on} (nM)	7.8 ± 3.7	50 ± 15

* $p < 0.001$ for t test comparison of (+)-tubocurarine versus pancuronium. Statistical comparisons were not performed for the Hill coefficient or calculated values (residency time and ℓ_{off}/ℓ_{on}).

In agreement with other researchers (Steinbach and Chen, 1995; Fletcher and Steinbach, 1996), we found that (+)-tubocurarine, but not pancuronium, acts as a partial agonist on embryonic mouse nAChR (single channel data not shown). (+)-Tubocurarine activates receptors in the absence of ACh and also increases channel activity at low concentrations of ACh. The latter effect is caused by activation of hetero-liganded receptors containing ACh at one binding site and (+)-tubocurarine at the other. The efficacy of both of these opening pathways is very low (Steinbach and Chen, 1995). In rapid perfusion experiments with 100 μM ACh, the baseline currents in the presence and absence of (+)-tubocurarine are indistinguishable. Thus, it is unlikely that these opening pathways interfere with out kinetic measurements.

We used the three-tube perfusion protocol to measure the kinetics of antagonist inhibition. In an onset experiment, a patch was exposed to a drug for varying intervals before application of ACh. The shortest interval that could reliably be attained was 10 ms. This allowed for rates <50/s to be measured; the fastest rate we observed in these experiments was 30/s. Pancuronium and (+)-tubocurarine have significantly different association rates: 2.7 and 1.2 $\times$ 10^8 M^{-1} s^{-1}, respectively. The drugs also differ in their dissociation rates: 2.1/s and 5.9/s, respectively. The kinetic results are consistent with the equilibrium results in that the ratio of dissociation rate to association rate is in good agreement with the IC_{50} values (Table 1).

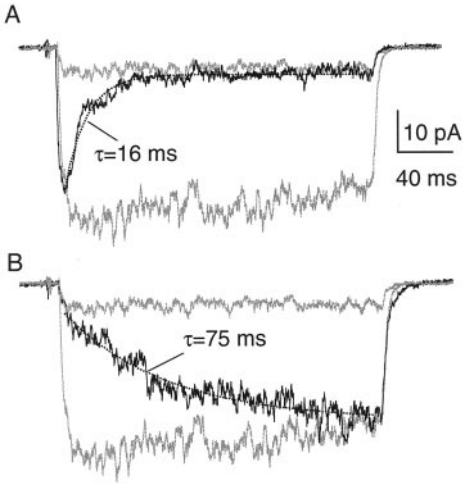

Fig. 4. The kinetics of inhibition by 400 nM curare revealed by different perfusion protocols with a nonsaturating concentration of ACh. 3 μM ACh, V = −50 mV. The gray traces are control and equilibrium exposure to curare. Black traces were fit to a single exponential decay; the time constants are indicated. A, the black trace was obtained by simultaneous perfusion of ACh and (+)-tubocurarine. B, the black trace was obtained by simultaneous perfusion of ACh and removal of (+)-tubocurarine.

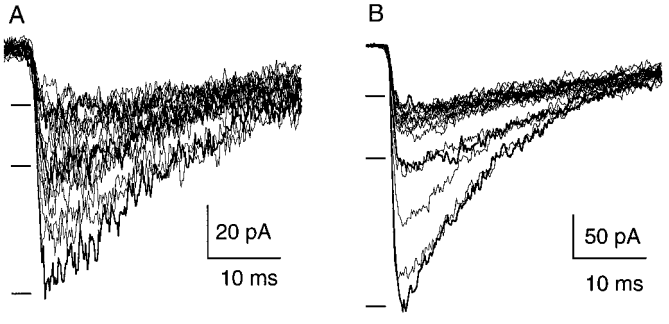

Fig. 5. Examples of onset kinetics obtained using the 3-tube perfusion system. A, family of 20 traces for 20 nM pancuronium. The three black traces are for 0-, 151-, and 428-ms exposure to pancuronium before application of 100 μM ACh. B, family of 20 traces for 150 nM (+)-tubocurarine. The three black traces are for 0-, 60-, and 428-ms exposure to (+)-tubocurarine before application of 100 μM ACh.

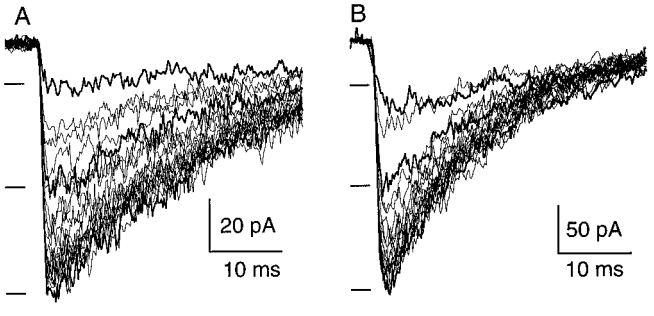

Fig. 6. Examples of recovery kinetics obtained using the 3-tube perfusion system. Data are from the same patches as shown in Fig. 5. A, family of 20 traces for 20 nM pancuronium. The three black traces are for 20, 341, and 1430 ms after removal of pancuronium before application of 100 μM ACh. B, family of 20 traces for 150 nM (+)-tubocurarine. The three black traces are for 20, 107, and 1050 ms after removal of (+)-tubocurarine before application of 100 μM ACh.

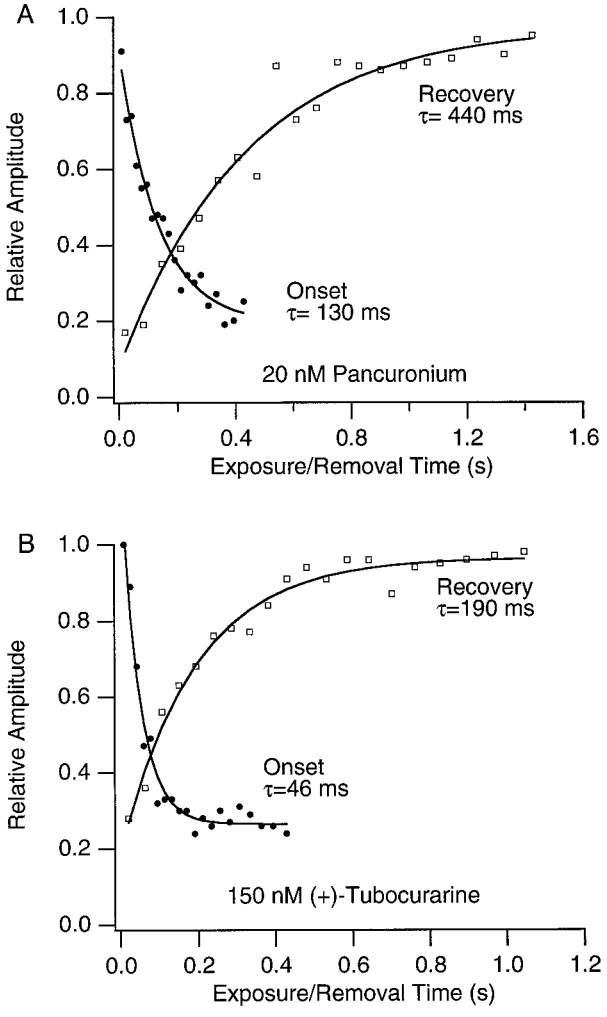

Fig. 7. The time course of onset and recovery of inhibition for 20 nM pancuronium (A) and 150 nM (+)-tubocurarine (B). Data are from the experiments shown in Figs. 5 and 6.

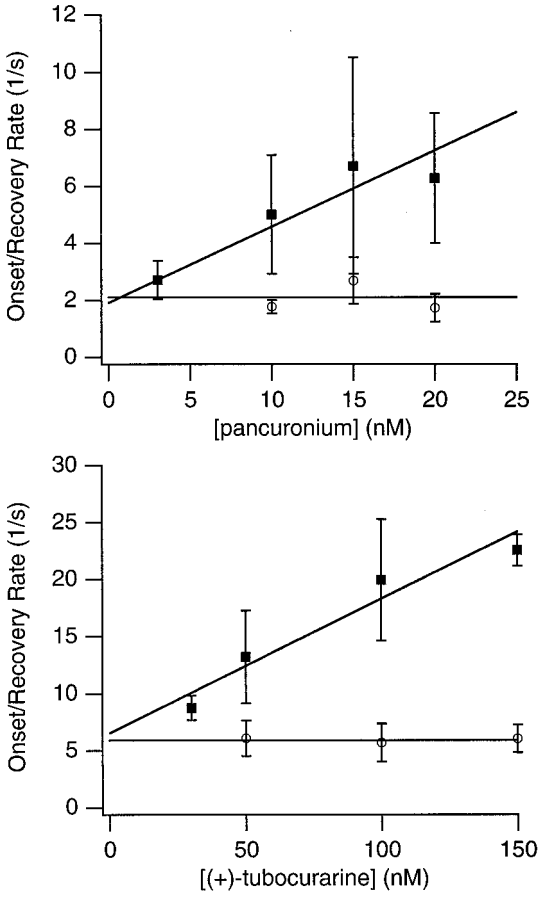

Fig. 8. The concentration-dependence of onset (■) and recovery (○) rates for pancuronium (A) and (+)-tubocurarine (B). The solid lines are fits of the data to eqs. 4 and 5. The fit parameters are given in Table 1.

These antagonist association rates are comparable with or greater than the association rate for ACh determined by single channel recording [embryonic, 4×10^7 M^{-1} s^{-1} (Zhang et al., 1995)[1]; adult, 1.7×10^8 M^{-1} s^{-1} (Akk and Auerbach, 1996)]. The agonist tetramethylammonium has an even slower association rate. It has been suggested that agonist binding is not diffusion limited (GulFreund, 1972) and may involve multiple interactions between agonist and protein before the binding site is reached (Zhang et al., 1995). Structural studies of the nAChR suggest the presence of narrow tunnels leading to agonist binding pockets within the α subunits (Miyazawa et al., 1999). Large antagonist molecules may not be able to diffuse freely through such tunnels. We hypothesize that antagonists prevent the access of agonists to the binding pocket by binding near the entrance to the tunnel. In this way, antagonists would reach their binding site without encountering the diffusion barriers seen by agonists. If bound agonist had a reciprocal effect on antagonist association, this model would mimic classical competitive antagonism.

Comparison of Our Kinetic Results with Results from Other Researchers. Measurements of ligand binding kinetics are complicated by fast desensitization. In addition, studies on tissue preparations may lead to apparent slow rates because of limited access of the ligand to its binding site. These problems may be overcome by using rapid perfusion techniques on small preparations. Ultimately, the resolution of the perfusion system determines the fastest rates that can be measured. The study by O'Leary et al. (1994) of (+)-tubocurarine binding to nAChR was limited by the speed with which a whole oocyte can be perfused. They noted that the observed recovery of currents from inhibition by (+)-tubocurarine had the same time course (3–5 s) as the bath exchange in their experimental setup. Aoshima et al. (1992) also used oocytes, but extracted kinetic information from the acceleration of desensitization after coapplication of agonist and antagonist. They estimated the dissociation of (+)-tubocurarine and pancuronium to be 70 and 39/s, respectively.

Colquhoun and Sheridan (1982) determined the dissociation rate of (+)-tubocurarine from frog muscle nAChR using a voltage jump protocol to change the closed-open channel equilibrium at 8°C. Carbachol was applied to the neuromuscular junction on the <1s time scale. The relaxation time constant increased from 2.2 to 3.4 ms in the presence of 400 nM (+)-tubocurarine. This suggests that dissociation of (+)-tubocurarine occurs on the 1 ms time scale; >100 times faster than our value. Extraction of the dissociation rate (1000/s) required modeling of nAChR kinetics. The association rate was calculated from this value and a measured equilibrium constant of 500 nM, yielding 10^9 M^{-1} s^{-1}. The disparity between these measurements and ours could be attributed to species differences. Comparison of the sequences of mouse and frog nAChR reveals a notable difference at residue 59 in the ϵ subunit. The mouse receptor has aspartic acid, whereas the frog has alanine. Bren and Sine (1997) studied the D59A mutant in mouse receptors (for unrelated reasons) and found that this mutation decreases the affinity of dimethyl tubocurarine by a factor of 25 (from 170 to 4300 nM). Although we did not use adult subtype ($\alpha_2\beta\epsilon\delta$) nAChR in our experiments, the (+)-tubocurarine affinities for embryonic and adult mouse nAChR are similar [71 and 61 nM, respectively (Steinbach and Chen, 1995)].[2]

Le Dain et al. (1991) also examined nAChR at the frog neuromuscular junction. They deduced the kinetics of (+)-tubocurarine by measuring miniature end-plate currents at 20°C and fitting these currents to a model of channel activation within a synapse. The (+)-tubocurarine dissociation constant was determined as 4000/s. This, coupled with an equilibrium inhibition constant of 4 μM (+)-tubocurarine, led to a calculated association rate of 8.9×10^8 M^{-1} s^{-1}. Again, the considerably higher dissociation rate found for frog compared with mouse may be attributed to species differences. In addition, study of an intact neuromuscular junction allows for presynaptic effects of (+)-tubocurarine to contribute to the observed responses.

The experiments of Bufler et al. (1996) most closely resemble ours in that they studied embryonic mouse nAChR in excised patches. They used myotubes rather than BC3H-1 cells. They measured the time course of recovery of currents after removal of 1 μM (+)-tubocurarine and found a 100-fold slower value for dissociation (0.1/s). Their perfusion system differed significantly from ours. They used a piezoelectric

[1] This low value for ACh association in embryonic receptors is incompatible with the fast activation on-rates measured at various concentrations of ACh in QF18 cells by Maconochie and Steinbach (1998). They used 2.5×10^8 M^{-1} s^{-1} in their simulations.

[2] The IC_{50} value for (+)-tubocurarine on adult mouse AChR expressed in human embryonic kidney 293 cells is 30 nM (our unpublished observations).

switching device to apply ACh rapidly but the change from (+)-tubocurarine–containing to (+)-tubocurarine–free solution was made with a stopcock 10 cm upstream from the outflow. They estimated that it required 100 ms to remove (+)-tubocurarine from the vicinity of the patch. In contrast, we used separate tubes for antagonist-free, antagonist-containing, and ACh-containing solutions. This minimized mixing delays so that antagonist was removed from the patch within 10 ms. However, differences in perfusion technique are not enough to account for the discrepancy between their results and ours. In addition, the equilibrium constant for (+)-tubocurarine determined by this group was 150 nM, 3-fold larger than ours. This group also reported on the kinetics of noncompetitive inhibition by >1 μM (+)-tubocurarine. However, their observation of an increased rate of current decay upon simultaneous application of ACh and high concentrations of (+)-tubocurarine is a manifestation of competitive inhibition (Aoshima et al., 1992) and may be only partly influenced by noncompetitive effects.

Our experiments differed from all previous studies in that we measured recovery at several antagonist concentrations, we measured onset and recovery, and we compared ℓ_{off}/ℓ_{on} with the independently measured equilibrium constants (Table 1). Our experiments and those of Bufler et al. (1996) represent a direct approach to the determination of antagonist kinetics, whereas others (Colquhoun and Sheridan, 1982; Le Dain et al., 1991) required modeling to deduce the dissociation rate.

Bufler et al. (1996) note correctly that high values of the (+)-tubocurarine association rate predict a significant decrease in peak current when ACh and (+)-tubocurarine are applied simultaneously. They observed a 20% decrease in peak current upon coapplication of 100 μM ACh with 100 μM (+)-tubocurarine and calculated that this was inconsistent with $\ell_{on} > 5 \times 10^6\ M^{-1}\ s^{-1}$. We also performed this experiment but found a 60% decrease in peak current upon coapplication. Simulations (not shown) suggest that this observation is consistent with a high (+)-tubocurarine association rate. However, these simulations are very sensitive to assumptions about the kinetics of the low affinity antagonist binding site about which nothing is currently known.

One question remains unanswered: we did not test quantitatively whether the biphasic current response seen in the presence of high (+)-tubocurarine concentrations is caused by fast dissociation of (+)-tubocurarine. The combination of antagonist, partial agonist, and hetero-liganded agonist actions of (+)-tubocurarine on embryonic receptors makes this system difficult to model. The companion article (Demazumder and Dilger, 2001) describes experiments with the nAChR antagonist cisatracurium. This drug exhibits a much larger biphasic current response than (+)-tubocurarine and does so in both embryonic and adult receptors. The article also demonstrates that ACh bound at one site may influence antagonist dissociation from the other site. The experimental results are in excellent agreement with an 11-state model for antagonist action and solidify the relationship between biphasic currents and antagonist dissociation.

Acknowledgments

We thank Claire Mettewie for maintenance of cell cultures, Ana Maria Vidal for performance of single channel experiments, Deeptankar Demazumder for helpful discussions, and Drs. Leon Moore and Chris Claussen for advice on statistical analyses.

References

Akk G and Auerbach A (1996) Inorganic, monovalent cations compete with agonists for the transmitter binding site of nicotinic acetylcholine receptors. *Biophys J* **70:**2652–2658.
Aoshima H, Inoue Y, and Hori K (1992) Inhibition of ionotropic neurotransmitter receptors by antagonists: Strategy to estimate the association and dissociation rate constant of antagonists with very strong affinity to the receptors. *J Biochem (Tokyo)* **112:**495–502.
Arias HR (2000) Localization of agonist and competitive antagonist binding sites on nicotinic acetylcholine receptors. *Neurochem Int* **36:**595–645.
Bren N and Sine SM (1997) Identification of the residues in the adult nicotinic acetylcholine receptor that confer selectivity for curariform antagonists. *J Biol Chem* **272:**30793–30798.
Brett RS, Dilger JP, Adams PR, and Lancaster B (1986) A method for the rapid exchange of solutions bathing excised membrane patches. *Biophys J* **50:**987–992.
Bufler J, Wilhelm R, Parnas H, Franke C, and Dudel J (1996) Open channel and competitive block of the embryonic form of the nicotinic receptor of mouse myotubes by (+)-tubocurarine. *J Physiol (Lond)* **495:**83–95.
Colquhoun D and Rang HP (1976) Effects of inhibitors of the binding of iodinated α bungarotoxin to acetylcholine receptors in rat muscle. *Mol Pharmacol* **12:**519–535.
Colquhoun D and Sakmann B (1981) Fluctuations in the microsecond time range of the current through single acetylcholine receptor ion channels. *Nature (Lond)* **294:**464–466.
Colquhoun D and Sheridan RE (1982) The effect of tubocurarine competition on the kinetics of agonist action on the nicotinic receptor. *Br J Pharmacol* **75:**77–86.
Corringer PJ, Le Novere N, and Changeux JP (2000) Nicotinic receptors at the amino acid level. *Annu Rev Pharmacol Toxicol* **40:**431–458.
Demazumder D and Dilger JP (2001) The kinetics of competitive antagonism by *cis*-atracurium of embryonic and adult nicotinic acetylcholine receptors. *Mol Pharmacol* **60:**797–807.
Dilger JP and Brett RS (1990) Direct measurement of the concentration- and time-dependent open probability of the nicotinic acetylcholine receptor channel. *Biophys J* **57:**723–731.
Dilger JP, Boguslavsky R, Barann M, Katz T, and Vidal AM (1997) Mechanisms of barbiturate inhibition of acetylcholine receptor channels. *J Gen Physiol* **109:**401–414.
Fletcher GH and Steinbach JH (1996) Ability of nondepolarizing neuromuscular blocking drugs to act as partial agonists at fetal and adult mouse muscle nicotinic receptors. *Mol Pharmacol* **49:**938–947.
Franke C, Hatt H, and Dudel J (1987) Liquid filament switch for ultra-fast exchanges of solutions at excised patches of synaptic membrane of crayfish muscle. *Neurosci Lett* **77:**199–204.
Gutfreund H (1972) *Enzymes: Physical Principles*. John Wiley & Sons, London.
Hamill OP, Marty A, Neher E, Sakmann B, and Sigworth FJ (1981) Improved patch-clamp techniques for high-resolution current recording from cells and cell-free membrane patches. *Pflueg Arch Eur J Physiol* **391:**85–100.
Hill AV (1909) The mode of action of nicotine and curari, determined by the form of the contraction curve and the method of temperature coefficients. *J Physiol (Lond)* **39:**361–373.
Jenkinson DH (1960) The antagonism between tubocurarine and substances which depolarize the motor endplate. *J Physiol (Lond)* **152:**309–324.
Le Dain AC, Madsen BW, and Edeson RO (1991) Kinetics of (+)-tubocurarine blockade at the neuromuscular junction. *Br J Pharmacol* **103:**1607–1613.
Liu Y and Dilger JP (1991) Opening rate of acetylcholine receptor channels. *Biophys J* **60:**424–432.
Maconochie DJ, Fletcher GH, and Steinbach JH (1995) The conductance of the muscle nicotinic receptor channel changes rapidly upon gating. *Biophys J* **68:**483–490.
Maconochie DJ and Knight DE (1989) A method for making solution changes in the sub-millisecond range at the tip of a patch pipette. *Pflueg Arch Eur J Physiol* **414:**589–596.
Maconochie DJ and Steinbach JH (1998) The channel opening rate of adult- and fetal-type mouse muscle nicotinic receptors activated by acetylcholine. *J Physiol (Lond)* **506:**53–72.
Miyazawa A, Fujiyoshi Y, Stowell M, and Unwin N (1999) Nicotinic acetylcholine receptor at 4.6 A resolution: transverse tunnels in the channel wall. *J Mol Biol* **288:**765–786.
O'Leary ME, Filatov GN, and White MM (1994) Characterization of d-tubocurarine binding site of *Torpedo* acetylcholine receptor. *Am J Physiol* **266:**C648–C653.
Parzefall F, Wilhelm R, Heckmann M, and Dudel J (1998) Single channel currents at six microsecond resolution elicited by acetylcholine in mouse myoballs. *J Physiol* **512:**181–188.
Rang HP (1966) The kinetics of action of acetylcholine antagonists in smooth muscle. *Proc R Soc Lond B Biol Sci* **164:**488–510.
Sine SM and Steinbach JH (1984) Activation of a nicotinic acetylcholine receptor. *Biophys J* **45:**175–185.
Sine SM and Taylor P (1981) Relationship between reversible antagonist occupancy and the functional capacity of the acetylcholine receptor. *J Biol Chem* **256:**6692–6699.
Steinbach JH and Chen Q (1995) Antagonist and partial agonist actions of D-tubocurarine at mammalian muscle acetylcholine receptors. *J Neurosci* **15:**230–240.
Tsuneki H, Kimura I, Dezaki K, Kimura M, Sala C, and Fumagalli G (1995) Immunohistochemical localization of neuronal nicotinic receptor subtypes at the pre- and postjunctional sites in mouse diaphragm muscle. *Neurosci Lett* **196:**13–16.
Unwin N (1995) Acetylcholine receptor channel imaged in the open state. *Nature (Lond)* **373:**37–43.
Zhang Y, Chen J, and Auerbach A (1995) Activation of recombinant mouse acetylcholine receptors by acetylcholine, carbamylcholine and tetramethylammonium. *J Physiol (Lond)* **486:**189–206.

Address correspondence to: James P. Dilger, Ph.D., Department of Anesthesiology, SUNY Stony Brook, Stony Brook, New York 11794-8480. E-mail: jdilger@epo.som.sunysb.edu